INTERNATIONAL JOURNAL FOR NUMERICAL METHODS IN FLUIDS
Int. J. Numer. Meth. Fluids 2005; **49**:999–1014
Published online 3 August 2005 in Wiley InterScience (www.interscience.wiley.com). DOI: 10.1002/fld.1037

Evaluation of adaptive mesh refinement and coarsening for the computation of compressible flows on unstructured meshes

Miguel A. T. Walter[1,‡], Aline A. Q. Abdu[1,§], Luís Fernando Figueira da Silva[1,*,†] and João Luiz F. Azevedo[2,¶]

[1]*Department of Mechanical Engineering, Pontifícia Universidade Católica do Rio de Janeiro, Rua Marquês de São Vicente, 225, Rio de Janeiro, RJ 22453-900, Brazil*
[2]*Institute of Aeronautics and Space, Centro Técnico Aeroespacial, CTA/IAE/ASE-N, São José dos Campos, SP 12228-904, Brazil*

SUMMARY

The compressible gas flows of interest to aerospace applications often involve situations where shock and expansion waves are present. Decreasing the characteristic dimension of the computational cells in the vicinity of shock waves improves the quality of the computed flows. This reduction in size may be accomplished by the use of mesh adaption procedures. In this paper an analysis is presented of an adaptive mesh scheme developed for an unstructured mesh finite volume upwind computer code. This scheme is tailored to refine or coarsen the computational mesh where gradients of the flow properties are respectively high or low. The refinement and coarsening procedures are applied to the classical gas dynamic problems of the stabilization of shock waves by solid bodies. In particular, situations where oblique shock waves interact with an expansion fan and where bow shocks arise around solid bodies are considered. The effectiveness of the scheme in reducing the computational time, while increasing the solution accuracy, is assessed. It is shown that the refinement procedure alone leads to a number of computational cells which is 20% larger than when alternate passes of refinement and coarsening are used. Accordingly, a reduction of computational time of the same order of magnitude is obtained.

KEY WORDS: unstructured grids; mesh adaption; compressible flows; finite volume

*Correspondence to: Luís Fernando Figueira da Silva, Department of Mechanical Engineering, Pontifícia Universidade Católica do Rio de Janeiro, Rua Marquês de São Vicente, 225, Rio de Janeiro, RJ 22453-900, Brazil.
†E-mail: luisfer@mec.puc-rio.br
‡E-mail: matwalter@hotmail.com
§E-mail: alineabdu@yahoo.com.br
¶E-mail: azevedo@iae.cta.br

Contract/grant sponsor: CNPq; contract/grant numbers: 501200/2003-7, 540109/2001-0

Received 1 February 2005
Revised 2 June 2005
Accepted 4 June 2005

1. INTRODUCTION

Mesh adaption procedures are frequently used to reduce the characteristic dimension of the computational cells in interesting regions of the flowfield, with the aim of yielding a better resolution of the simulated phenomena. Most often in computational fluid dynamics, such regions are those where the gradients of the flow properties are high or where the numerical solution exhibits a large error. Typical regions of high gradients are boundary and shear layers, chemical reaction fronts and shock waves. The exact position of these regions are not known *a priori*. In particular, shock waves are usually captured by the discretization schemes of the governing equations and span over two or three computational cells, even though the physical dimension of these waves is of the order of a few mean free paths of the gas molecules.

Successive refinements are usually necessary to achieve a good resolution of the regions of the flowfield where high gradients occurs. As a consequence, a significant increase of the number of mesh volumes may result, eventually leading to a concentration of refined volumes in regions of the flowfield where those volumes are no longer needed. Thus, mesh coarsening techniques are of interest with the aim of increasing the characteristic dimension of the computational mesh, ultimately leading to a reduction of the computational time.

In this paper refinement and coarsening techniques tailored for unstructured meshes will be evaluated with respect to the gains in solution accuracy and computational time. During the past few years, several authors have developed mesh adaption techniques in an unstructured mesh context.

Hierarchical mesh adaption techniques have been developed by Kallinderis and Vijayan [1] and Speares and Berzins [2] on three-dimensional unstructured meshes. The refinement procedure leads to a nested mesh structure, in which the previous coarse mesh is stored adjacent to the refined one. The coarsening procedure acts only in regions previously refined, and thus the coarsest mesh possible is the original mesh. Therefore, the largest spatial scales are fixed by the choice of the initial mesh.

Dompierre *et al.* [3] and Webster *et al.* [4] have developed a technique based on the collapse of edges in order to coarsen unstructured meshes in two-dimensional configurations. In this method, the nodes which define a given edge are transformed in one node, and the volumes around the removed edge cease to exist. Figure 1 provides a schematic representation of this situation.

While the former method is better suited for the simulation of transient phenomena, since the initial (coarsest) mesh can be recovered at any time, the latter is more indicated to the simulation of steady state problems. Moreover, the edge-based data structure used in the computer code adopted in the present work [5–7] is ideally suited to the edge-collapse technique.

Miller *et al.* [8] developed a coarsening approach for two-dimensional unstructured meshes which leads to a sequence of bounded aspect ratio meshes, i.e. meshes for which all elements have bounded aspect ratios. This procedure guarantees that both the number of meshes in the sequence and the number of elements on a given mesh are optimal. Another procedure, which may be used to coarsen the mesh, begins with the choice of one node to be removed. As illustrated in Figure 2, around this node a diagonal swap technique is applied in order to end up with only three edges sharing this node. These edges are removed, together with the three adjoining triangles, and a new triangle is formed.

Still another possibility, which has not been explored in the literature, to the best of the authors' knowledge, is the use of Delaunay triangulations to reconstruct regions of the mesh

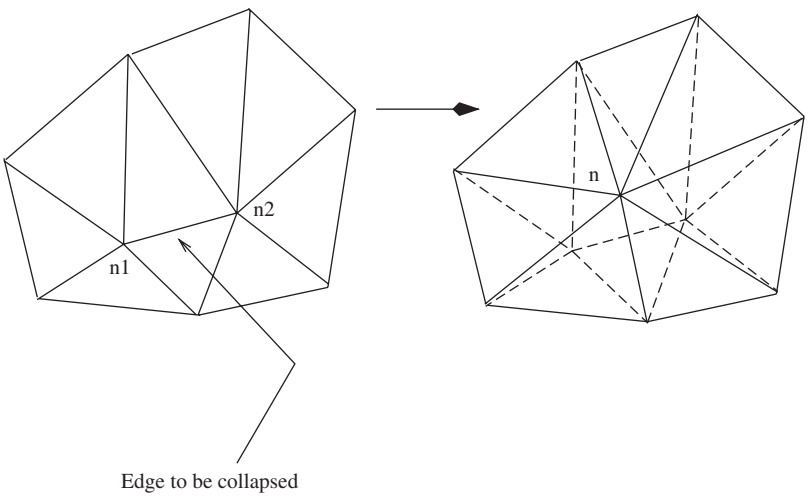

Figure 1. Coarsening scheme using the edge-collapse procedure.

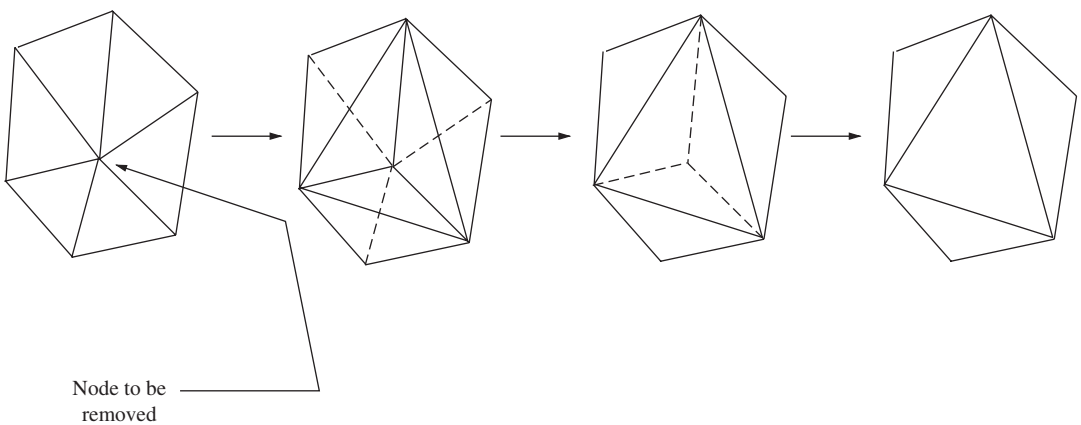

Figure 2. Diagonal swap coarsening procedure.

where triangles have been removed. This procedure does not necessarily lead to an increase of the characteristic dimension of the mesh. Moreover, the Delaunay triangulation complicates the attribution of properties from the original mesh to the new one. Finally, sophisticated implementations could be devised, which would combine two or more of the techniques briefly described here, with the aim of optimizing the mesh quality. However, defining such implementations is beyond the scope of the present work.

After recalling the mathematical formulation for 2-D gas dynamic problems, and the associated numerical method, the paper describes in detail the mesh coarsening procedure developed. Then the refinement/coarsening procedure is evaluated by means of computations of three compressible gas flow problems.

2. THEORETICAL FORMULATION

In the present case, the flowfield is simulated using the 2-D Euler equations, which can be written in integral conservative form for a 2-D coordinate system as

$$\iint_V \frac{\partial \mathbf{U}}{\partial t}\,\mathrm{d}x\,\mathrm{d}y + \int_S (\mathbf{F}\,\mathrm{d}y - \mathbf{G}\,\mathrm{d}x) = \iint_V \mathbf{Q}\,\mathrm{d}x\,\mathrm{d}y \tag{1}$$

The vector of conserved quantities, **U**, the expressions for the convective flux vectors, **F** and **G**, and the chemical source vector, **Q**, are written as

$$\mathbf{U} = \begin{bmatrix} \rho \\ \rho u \\ \rho v \\ \rho E \\ \rho Y_1 \\ \rho Y_2 \\ \vdots \\ \rho Y_{N-1} \end{bmatrix}, \quad \mathbf{F} = \begin{bmatrix} \rho u \\ \rho u^2 + p \\ \rho uv \\ u(\rho E + p) \\ \rho Y_1 u \\ \rho Y_2 u \\ \vdots \\ \rho Y_{N-1} u \end{bmatrix}, \quad \mathbf{G} = \begin{bmatrix} \rho v \\ \rho uv \\ \rho v^2 + p \\ v(\rho E + p) \\ \rho Y_1 v \\ \rho Y_2 v \\ \vdots \\ \rho Y_{N-1} v \end{bmatrix}, \quad \mathbf{Q} = \begin{bmatrix} 0 \\ 0 \\ 0 \\ 0 \\ \dot{\omega}_1 W_1 \\ \dot{\omega}_2 W_2 \\ \vdots \\ \dot{\omega}_{N-1} W_{N-1} \end{bmatrix} \tag{2}$$

The nomenclature used in this system of equations is the one usually adopted in aerospace applications, such that ρ is the density, u and v are the Cartesian velocity components, E is the total energy per unit of mass, Y_i, $\dot{\omega}_i$, W_i are the mass fraction, the molar production rate, and the molecular weight of the ith species, respectively, and p is the static pressure.

In the solution of Equation (1), $N-1$ chemical species are necessary, since the mass fraction of the last chemical species, Y_N, is calculated as $Y_N = 1 - \sum_{i=1}^{N-1} Y_i$. The state equation for a mixture of thermally perfect gases

$$p = \rho \mathscr{R} T \sum_{i=1}^{N} \frac{Y_i}{W_i} \tag{3}$$

is used to evaluate the pressure, p. In this equation, $\mathscr{R}$ is the universal gas constant. The total energy, E, is defined as the sum of the internal energy and the kinetic energy,

$$E = e + \frac{1}{2}(u^2 + v^2) = \sum_{i=1}^{N} Y_i e_i + \frac{1}{2}(u^2 + v^2) = \sum_{i=1}^{N} Y_i h_i - \frac{p}{\rho} + \frac{1}{2}(u^2 + v^2) \tag{4}$$

The internal energy is a function of the mixture composition and of the temperature, T, which is calculated by a Newton method once e is known. This is required since the specific enthalpy of the species are represented by 5th-order polynomials of the temperature in the present case [9]. Note that, although the formulation above is pertinent to variable mixture composition flows of interest to previous studies [6, 7, 10], the results presented here consider air as the working fluid.

3. NUMERICAL METHOD

Computations are performed using a numerical code [6] that solves the governing equation system given in Equations (1) and (2) using an upwind cell-centred finite volume method on unstructured triangular meshes. Temporal discretization uses a classical, 2nd-order, Runge–Kutta time stepping scheme [11]. In the spatial discretization, the interface fluxes are formulated using the Advection Upstream Splitting Method ($AUSM^+$ [12]). Spatial higher order accuracy is sought with MUSCL [13] extrapolation. This code has been validated against analytical and experimental results for several compressible gas flows [5–7, 10].

4. ADAPTIVE REFINEMENT

The adaptive mesh refinement technique used [6] increases the number of grid points in regions of the flowfield where large property gradients occur. The procedure requires the identification of such regions, which is accomplished based on a sensor quantity defined for each computational cell

$$(\text{sensor})_i = \max_m \left(\frac{|\nabla \zeta_m|_i}{|\zeta_{m_{\max}} - \zeta_{m_{\min}}|} \right), \quad \zeta_m = (p, u, v, T, Y_j) \tag{5}$$

where $\zeta_{m_{\max}}$ and $\zeta_{m_{\min}}$ are the maximum and the minimum values of the ζ_m property in the whole flowfield and $|\nabla \zeta_m|_i$ is the magnitude of the gradient of the ζ_m property in the ith control volume. As described in greater detail elsewhere [6], the refinement procedure halves the faces of each volume for which the sensor exceeds a prescribed threshold. The new node created is connected either to existing or to new nodes, leading to the formation of two or four smaller triangles, respectively. Successive refinements are typically used to obtain an adequate resolution of shock or detonation waves [6, 7, 10]. However, as several passes of refinement are used, and flow structures steepen, regions of the flowfield may arise where an unnecessary concentration of computational volumes appears. This drawback of the application of the refinement process to the problems of interest to the authors prompted the development of the following coarsening procedure.

5. COARSENING PROCEDURE

The coarsening procedure used in this work is based on the edge collapse technique, illustrated in Figure 1. The procedure consists on the collapse of two adjoining nodes (n_1 and n_2), leading to the formation of a new node (n). As a result of this procedure, the two neighbouring volumes are removed.

5.1. The node removal process

Starting from the computed results on the initial mesh, Equation (5) is used to calculate the normalized gradients of the selected variables in the computational domain. The gradients on the edges are calculated as the average of the gradients of the neighbouring volumes of a given edge. The edges which have a value of the normalized gradient below a given threshold are

chosen as possible candidates to be removed. These nodes are ordered in a list by increasing values of the gradient. The selected edge removal will occur only if the new mesh quality would not be reduced when compared to the original one. The mesh quality measure will be discussed further on.

Note that the quality of resulting volumes depends on the position of the new node. As shown in Figure 3, the procedure considers the following positions:

1. The geometric centre of the polygon formed by all volumes surrounding the node, Figure 3(a).
2. The centre of the edge to be collapsed, Figure 3(b).
3. Each one of the two original nodes of the edge, Figures 3(c) and (d).

The position which leads to the best quality of the modified volumes is chosen. If none of these locations yields a good mesh quality, this edge is deleted from the list of edges to be removed.

Once an edge has been chosen for removal, and with the purpose of avoiding an excessive growth of the volumes, it is enforced that no edges of the same volume will be chosen for removal in the current coarsening pass. As a consequence, a given node is not allowed to be displaced twice during a pass of the coarsening procedure. This restriction defines a domain of influence corresponding to the edge that will be removed, as shown in Figure 4. All the neighbouring edges of a node that belong to an edge selected to be removed are deleted from the list of edges to be removed, regardless of the value of the sensor.

Special care is needed for coarsening volumes along a computational boundary. The present procedure does not consider the removal process in boundary edges, since the code does not contain geometric information about the boundaries. Furthermore, for the edges that have one node at the boundary, the only possible result would be the collapse to the boundary node,

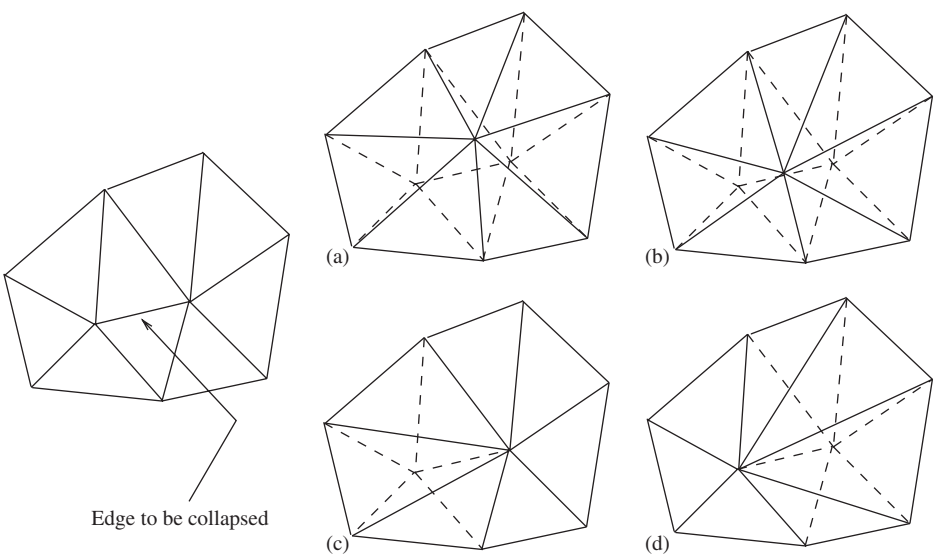

Figure 3. Representation of the four different possibilities of the edge collapse.

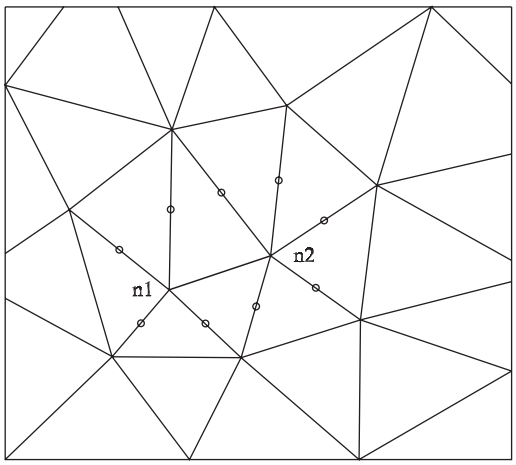

Figure 4. Influence domain of the collapsed edge.

since the edges which define the contour cannot be changed. Therefore, the current implementation does not consider the collapse of edges which have at least one node at the boundary, since it would not lead to a significant increase of the characteristic length scale of the computational mesh. One should note that the drawback related to fixing the edges which have a node at a boundary is not large, as the number of edges at the boundaries is much smaller than those at the interior of the computational domain, at least for the cases of interest in this work.

Once the edge removal process is finished, the mesh data structure has been modified, leading to the absence of nodes and volumes. In the present context of cell-centred finite volume method, reordering and renumbering the position, connectivity, neighbouring and boundary volume tables are necessary. The attribution of the volume properties occurs, simultaneously, as the volume reordering proceeds. Since the presented applications concern only the removal of edges in regions of the flowfield where gradients are relatively small, on the current implementation the properties of the modified volumes remain unchanged. If one is interested in removing edges in high gradient regions, more sophisticated procedures should be used in which the properties of each of the modified volumes are altered to enforce conservation. Figure 3 suggests that such a procedure could be based on volume averages, in which a modified volume receives part of the mass, momentum and energy of the original volumes that are overlaid.

The ordering process uses two types of lists. The first one is the list of removed nodes, which has dimension equal to 2φ and increasingly orders the removed nodes (n_1 and n_2). The second is the new node list, with dimension φ, which has the number of each new node (n) and the number of the volumes which share those vertices. One should note that the number of the new nodes is half the number of removed nodes. The reordering position table is created by direct attribution of the number of the first φ removed nodes to the new nodes, with simultaneous update of the coordinates. For the last φ nodes, starting by the last element of the list of removed nodes, a shift up movement has to be executed. The reconstruction of the neighbourhood table and boundary volume table is performed by the position reordering table and connectivity table.

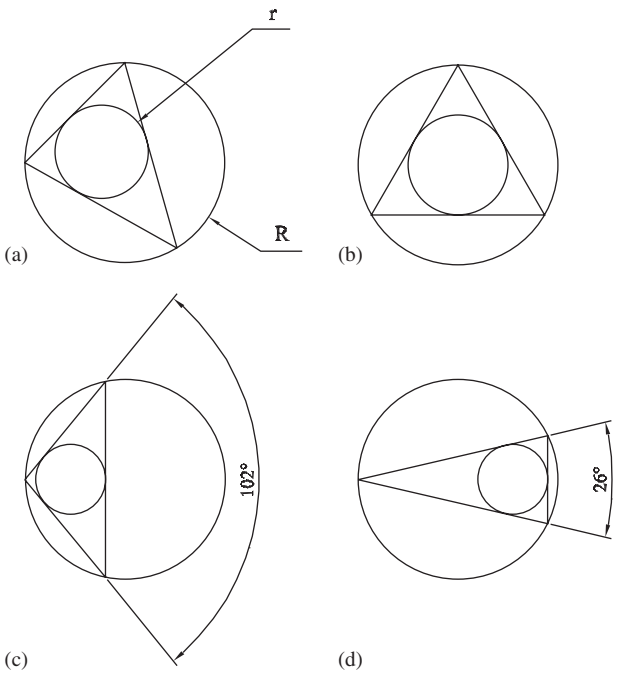

Figure 5. Scheme of volumes with different values of Q_Δ.

5.2. The quality measure

In this work, the quality of the volumes is a measure of the elongation of the triangles, defined as the ratio of the radius of the inscribed and circumscribed circles

$$Q_\Delta = 2\frac{r}{R}$$

where r and R are the radii of the inscribed and circumscribed circles of the triangle, respectively, as shown in Figure 5(a). The quality criterion adopted in the mesh coarsening procedure is defined by

$$C \leqslant Q_\Delta \leqslant 1$$

It should be noted that, for an equilateral triangle (Figure 5(b)), $Q_\Delta = 1$. The value of the constant C indicates the minimum quality value accepted. Good results have been obtained with C around 0.70–0.75. As an illustration of this metric, note that isosceles triangles with angles equal to 26° and 102°, shown in Figures 5(c) and (d), respectively, both have values of quality $Q_\Delta = 0.70$.

6. RESULTS AND DISCUSSION

The mesh adaption procedure has been tested in three supersonic airflow configurations. The first configuration analysed is the forward facing step subject to a supersonic air flow. In

this classical configuration only the mesh coarsening procedure has been applied. The second configuration involves the stabilization of an oblique shock wave (OSW) around a compression ramp, whereas the third considers a ramp of finite length which leads to the interaction between the OSW and an expansion fan. For these last two cases, the results obtained with a coarse mesh are compared to those obtained (i) when three passes of the adaption procedure are performed after convergence of the computations and (ii) when, in addition to these three refinement passes, mesh coarsening is performed a few interactions prior to refinement. The time required to perform mesh refinement and coarsening is clearly a function of the values of the adaption thresholds required, i.e. the larger the number of cells to be refined or edges to be collapsed, the longer the computational time. In all cases presented in this paper, the cost of a refinement or coarsening pass is at most equal to that of a single time step. All the computations have been performed on a Pentium IV, 2.4 MHz processor using Linux RedHat 9.0 distribution and the Gnu compiler.

6.1. *Boundary conditions*

The boundary conditions used in this work are classical. Since all the cases studied concern supersonic flows, at the entrance of the computational domain fixed values of Mach number, pressure and temperature are prescribed for the air flows. The incoming flow is always parallel to the x-axis. These flow conditions are adopted as initial conditions throughout the computational domain. When solid walls are present, adiabatic, non-catalytic, slip boundary conditions are used. Symmetry conditions are imposed at $y = 0$. Concerning the exit boundaries, non-reflective characteristic boundary conditions are used [14].

6.2. *Forward facing supersonic step*

The supersonic forward facing step is a classical configuration used for evaluating computational fluid dynamics schemes [15]. The freestream flow Mach number, $M_\infty = 3$, is the one corresponding to the computational results obtained by Woodward and Colella [15], although the focus here is not on the accuracy of the computations. The evolutions of density and pressure on this flowfield are given in Figure 6 for the finest mesh used, which considers a quasi-regular triangular distribution, where each boundary is divided in segments of length equal to $\frac{1}{80}$th of the height of the computational domain. This figure clearly shows the distinct bow shock wave that stabilizes upstream of the step as well as the subsequent Mach reflections and interactions between oblique shock waves, expansion fans, and shear layers.

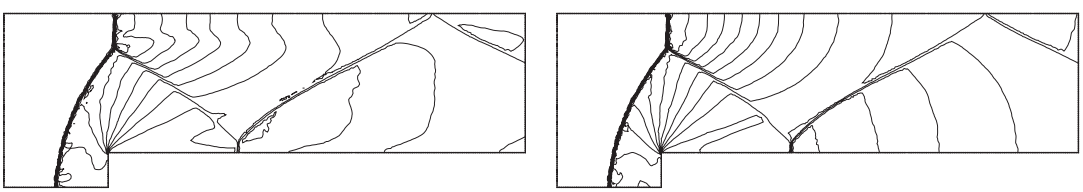

Figure 6. Density and pressure contours for a $M_\infty = 3$, $p_\infty = 1$ atm, $T_\infty = 300$ K, flow over a forward facing step.

The goal here is to evaluate the performance of the mesh coarsening procedure previously described. Thus, the results obtained on the fine mesh are compared to computations for which coarsening of successively larger thresholds are considered. Three coarsening passes are performed after convergence of the solution is obtained. Table I gives the values of the thresholds used in each pass. Note that, for all the computed results, 4000 interactions have been performed, and that the three coarsening passes occur at interactions 300, 1000 and 2000. In this table, the final number of nodes and triangles are also given, as well as the total CPU time required for the computations. The table shows that the gains in CPU time, which span from 15 to 20% as the mesh is coarsened, are smaller than those obtained in storage space, which reach 27% for the coarsest mesh. This is natural, since convergence is first obtained on a fine mesh before coarsening is applied.

The effect of the coarsening procedure on the computed solution can be assessed in Figure 7. In this figure the evolutions of pressure and Mach number along a horizontal line placed at the initial half-height of the channel are shown, for the seven cases listed in Table I. The crossing of the shock waves and subsequent flow expansions can be clearly distinguished. The use of the coarsening procedure is found to lead to practically no degradation of the

Table I. Comparison of the different mesh coarsening cases for the forward-facing step problem.

Case number	Thresholds	Number of nodes (% reduction)	Number of elements (% reduction)	CPU time (s) (% reduction)
0	(0.0, 0.0, 0.0)	20124 (—)	39606 (—)	57746 (—)
1	(0.1, 0.1, 0.1)	16066 (20.2)	31490 (20.5)	48788 (15.5)
2	(0.1, 0.2, 0.2)	16004 (20.5)	31366 (20.8)	48555 (15.9)
3	(0.1, 0.3, 0.3)	15786 (21.6)	30930 (21.9)	48254 (16.4)
4	(0.1, 0.4, 0.4)	15438 (23.3)	30234 (23.7)	47142 (18.4)
5	(0.1, 0.5, 0.5)	15047 (25.2)	29452 (25.6)	46326 (19.8)
6	(0.1, 0.6, 0.6)	14608 (27.4)	28574 (27.9)	46096 (20.2)

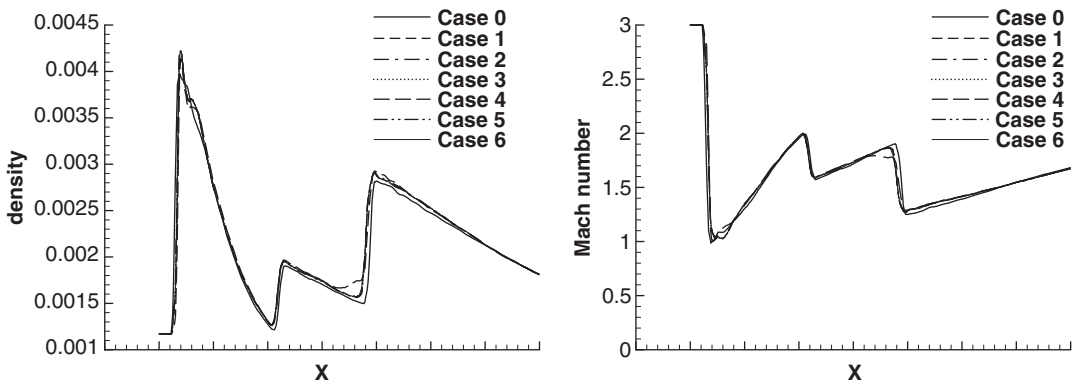

Figure 7. Density (g/cm^3) and Mach number evolution at half-height for a $M_\infty = 3$, $p_\infty = 1$ atm, $T_\infty = 300$ K, flow over a forward facing step.

solution quality. Indeed, this figure shows that a very good agreement is obtained between the computed results. The exception lies at the crossing of the last shock wave, where discrepancies that may reach 10% of the local density value are observed due to the smearing of the shock wave that occurs at the coarser meshes.

6.3. *Two-dimensional supersonic wedge*

Figure 8 gives the results of the computations performed for the second configuration using, as freestream parameters, $M_\infty = 2.25$, $T_\infty = 300\,\mathrm{K}$ and $p_\infty = 1\,\mathrm{atm}$. The value of the wedge angle is $\delta = 20°$, and the freestream is aligned with the x-direction. In this figure the resulting meshes and the pressure contours are shown. The results of the mesh refinement and coarsening procedures can be clearly seen in this figure. The value of the sensor threshold used in all refinement passes is 0.01, whereas the coarsening procedure uses 0.75. Note that mesh adaption is performed after convergence of the computation is obtained on a given mesh. The initial mesh, which is shown in Figure 8(a), contains 751 nodes and 1391 volumes. The mesh which results from three refinement passes is shown in Figure 8(b), and has 3630 nodes and 7120 volumes. In this case, the total computational time is 6.0 h. The mesh and the solution corresponding to three refinement and two coarsening passes is given in Figure 8(c). The final number of nodes and volumes is 2843 and 5552, respectively, and the total CPU time is 4.8 h. Note that this computational time includes the elapsed time during the refinement and coarsening passes. Thus, the use of mesh coarsening, in addition to mesh refinement, led to a reduction of 22% in the number of volumes and of 20% in the CPU time, when compared to using mesh refinement alone.

6.4. *Supersonic finite ramp*

The results obtained for the finite ramp configuration are shown in Figure 9. The ramp used has an angle of $\delta = 40°$, and the freestream flow parameters are $M_\infty = 8$, $T_\infty = 300\,\mathrm{K}$ and $p_\infty = 1\,\mathrm{atm}$. In this figure, the final mesh and pressure fields for the initial mesh are shown for the case of three refinement passes and for the case where two coarsening passes precede the last two refinements. The threshold values used in the refinement and coarsening passes are the same as those used in the wedge cases. The initial mesh, shown in Figure 9(a) contains 1105 nodes and 2065 volumes, whereas the mesh resulting from three refinement passes, which is depicted in Figure 9(b), contains 6500 nodes and 12 798 volumes. The total CPU time in the latter case is 8.5 h. Figure 9(c) gives the results obtained when two coarsening passes are also performed. The final mesh, for which the total computational time was 6.9 h, has 5262 nodes and 10 322 volumes. In this case, the reduction in CPU time is 18.8%, and the number of volumes was decreased 19.3%.

The computed flow solution is not affected by the coarsening procedure, as it could be expected. This is illustrated in Figure 10 by the longitudinal evolution of different flow properties, which are taken along the '0' line. This figure shows that a clear improvement of the shock wave resolution results when the mesh is refined. Indeed, the values of pressure and temperature predicted by the shock polar analysis [16], 47.4 atm and 2325 K, could not be reproduced by the calculation on the initial coarse mesh. After the three refinement passes, the computed values exhibit an excellent agreement with the classical analysis. Moreover, the use of the coarsening procedure does not alter the pressure downstream of the oblique shock wave, and only minor differences are observed in the flow expansion region.

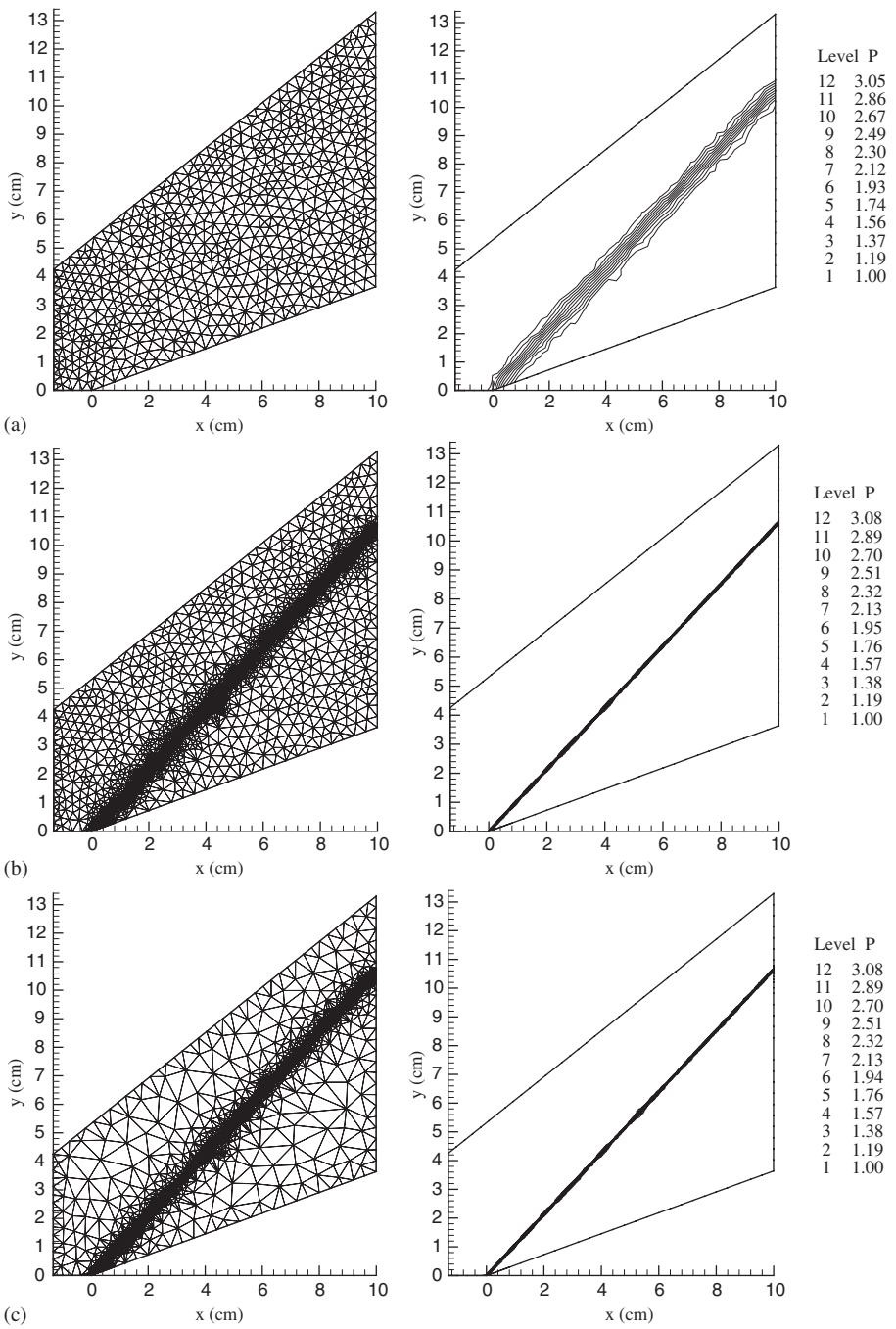

Figure 8. Mesh and pressure field (atm) corresponding to the airflow around a compression ramp, $M_\infty = 2.25$, $T_\infty = 300\,\mathrm{K}$ and $p_\infty = 1\,\mathrm{atm}$, wedge angle $\delta = 20^\circ$.

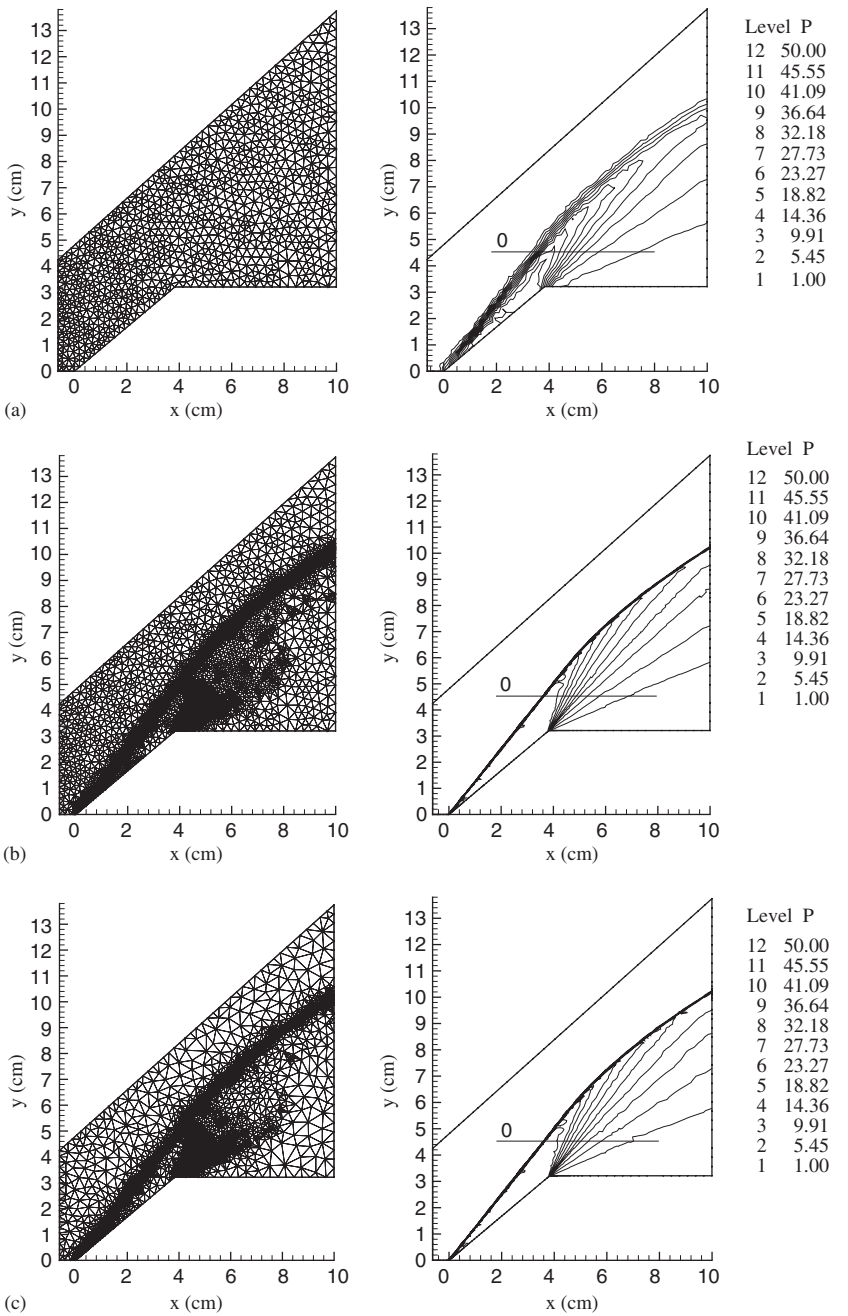

Figure 9. Mesh and pressure field (atm) corresponding to the airflow around a compression/expansion ramp, $M_\infty = 8$, $T_\infty = 300\,\mathrm{K}$ and $p_\infty = 1$ atm, wedge angle $\delta = 40^\circ$.

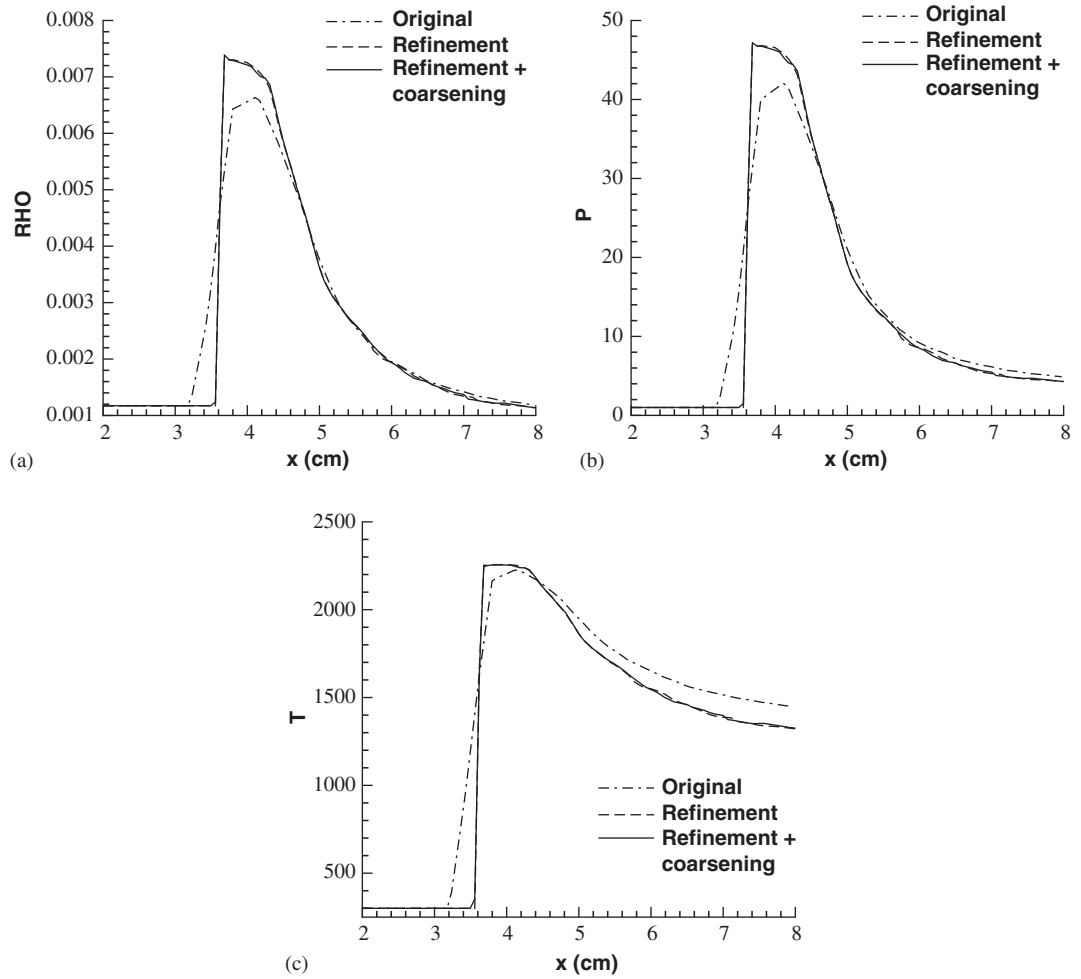

Figure 10. Longitudinal evolutions of density (g/cm^3), pressure (atm) and temperature (K) along the '0' line shown in Figure 9: (a) density; (b) pressure; and (c) temperature.

7. CONCLUSIONS

This paper has presented a grid coarsening procedure that can be used for general triangular unstructured grids. The procedure was constructed in such a way as to guarantee that the mesh quality is not degraded as the grid is coarsened and that the costs of both refinement and coarsening procedures are equivalent to that of a single time step. The coarsening procedure was implemented in a code which already had the capability to perform adaptive mesh refinement. The work was developed in the context of providing a computational tool that can be used to simulate high speed flows and, in particular, supersonic combustion flows. For such cases, successive mesh refinements are typically used to achieve the desired resolution

of shock or detonation waves. However, the use of successive refinements eventually leads to an unnecessary concentration of the mesh in flow regions in which there are no more high gradients, which can constitute a waste of computational resources. Hence, the availability of both refinement and coarsening capabilities yields the possibility of analysing reactive flow regimes previously unattainable to the authors due to high computational costs.

The test cases considered in the paper have addressed typical configurations for high speed gas dynamic problems. The results have shown that the proposed coarsening procedure is effective in reducing computational costs without affecting the quality of the solutions obtained. In particular, the results have shown that the resolution of shock and contact surfaces is not affected by the mesh coarsening. For the test cases considered in the present work, the results have indicated on the order of 20% storage and computational time savings after three passes of the refinement/coarsening procedures, when compared to computations which used mesh refinement alone. Furthermore, as the results also indicated, such savings were achieved without compromising the quality of the computational meshes.

Even if the present adaptive mesh scheme has been applied to flowfields described by the Euler equations, the essence of the refinement/coarsening procedure does not depend on the particular physical formulation being solved. Clearly, when addressing viscous computations, one may want to investigate combinations of variables that would be more adequate for the sensor definition.

Future work should involve the implementation of multigrid together with adaptive meshing. Indeed, there are other versions of the present code [17] which have implemented multigrid techniques. As a final remark, note that the extension of the technique presented to generalized three-dimensional meshes is object of future work. In particular, issues associated to the removal of cell faces and to a measure of quality for generalized polyhedrons need to be examined.

ACKNOWLEDGEMENTS

During this work L. F. Figueira da Silva was on leave from *Laboratoire de Combustion et de Détonique*, *Centre Nacional de la Recherche Scientifique*, France, with a PROFIX scholarship from CNPq-Brazil. M. A. T. Walter thanks FAPERJ (*Fundação Carlos Chagas Filho de Amparo à Pesquisa do Estado do Rio de Janeiro*) for his scholarship. The authors also gratefully acknowledge the partial support of CNPq through the Integrated Project Research Grant nos. 501200/2003-7 and 540109/2001-0.

REFERENCES

1. Kallinderis Y, Vijayan P. Adaptive refinement-coarsening scheme for three-dimensional unstructured meshes. *AIAA Journal* 1993; **31**(8):1440–1447.
2. Speares W, Berzins M. A 3D unstructured mesh adaption algorithm for time-dependent shock-dominated problems. *International Journal for Numerical Methods in Fluids* 1997; **25**(1):81–104.
3. Dompierre J, Labbé P, Garon A, Camarero R. Unstructured tetrahedral mesh adaption for two-dimensional space-time finite elements. *AIAA 38th Aerospace Sciences Meeting and Exhibit*, American Institute of Aeronautics and Astronautics, 2000, *AIAA Paper 2000-0810*.
4. Webster BE, Shephard MS, Rusak Z, Flaherty JE. Automated adaptive time-discontinuous finite element method for unsteady compressible airfoil dynamics. *AIAA Journal* 1994; **32**(4):748–757.
5. Figueira da Silva LF, Azevedo JLF, Korzenowski H. On the development of an unstructured grid solver for inert and reactive high speed flow simulations. *RBCM—Journal of the Brazilian Society of Mechanical Sciences* 1999; **XXI**(4):564–579.
6. Figueira da Silva LF, Azevedo JLF, Korzenowski H. Unstructured adaptive grid flow simulations of inert and reactive gas mixtures. *Journal of Computational Physics* 2000; **160**(2):522–540.

7. Pimentel CAR, Azevedo JLF, Figueira da Silva LF, Deshaies B. Numerical study of wedge supported oblique shock wave-oblique detonation wave transitions. *Journal of the Brazilian Society of Mechanical Sciences* 2002; **XXIV**(3):149–157.
8. Miller GL, Talmor D, Tseng SH. Optimal coarsening of unstructured meshes. *Journal of Algorithms* 1999; **31**(1):29–65.
9. Kee RJ, Rupley FM, Miller JA. CHEMKIN-II: a Fortran chemical kinetics package for the analysis of gas phase chemical kinetics. *SAND89-8009B/UC-706*. Sandia National Laboratories: Albuquerque, NM, 1991.
10. Walter MAT, Figueira da Silva LF. Numerical study of detonation stabilization by finite length wedges. *43rd AIAA/ASME/SAE/ASEE Joint Propulsion Conference and Exhibit*, American Institute of Aeronautics and Astronautics, 2004, *AIAA Paper 2004-3712*.
11. Mavriplis DJ. Multigrid solution of the two-dimensional Euler equations on unstructured triangular meshes. *AIAA Journal* 1988; **26**(7):824–831.
12. Liou MS. A sequel to AUSM: AUSM$^+$. *Journal of Computational Physics* 1996; **129**(2):364–382.
13. Hirsch C. *Numerical Computations of Internal and External Flows*, vol. 2. Wiley: Chichester, 1990.
14. Thompson KW. Time dependent boundary conditions for hyperbolic systems. *Journal of Computational Physics* 1987; **68**(1):1–24.
15. Woodward P, Colella P. The numerical simulation of two-dimensional fluid flow with strong shocks. *Journal of Computational Physics* 1984; **54**(1):115–173.
16. Shapiro AH. *The Dynamics and Thermodynamics of Compressible Fluid Flow*. Robert E. Krieger: Malabar, FL, 1983.
17. Strauss D, Azevedo JLF. Unstructured multigrid simulations of turbulent launch vehicle flows including a propulsive jet. *Journal of Spacecraft and Rockets* 2004; **41**(5):745–753.

